

PAPER • OPEN ACCESS

Structural study of thick hexaferrite films

To cite this article: T Koutzarova *et al* 2020 *J. Phys.: Conf. Ser.* **1492** 012064

View the [article online](#) for updates and enhancements.



IOP | ebooks™

Bringing together innovative digital publishing with leading authors from the global scientific community.

Start exploring the collection—download the first chapter of every title for free.

Structural study of thick hexaferrite films

**T Koutzarova^{1,5}, B Georgieva¹, S Kolev¹, Ch Ghelev¹, K Krezhov¹,
D Kovacheva², B Vertruyen³, R Closset³, L-M Tran⁴ and A Zaleski⁴**

¹Acad. Emil Djakov Institute of Electronics, Bulgarian Academy of Sciences
72 Tzarigradsko Chaussee, 1784 Sofia, Bulgaria

²Institute of General and Inorganic Chemistry, Bulgarian Academy of Sciences,
Acad. Georgi Bonchev Str., Bld. 11, 1113 Sofia, Bulgaria

³Greenmat, Chemistry Department, University of Liege,
11 allée du 6 août, 4000 Liège, Belgium

⁴Institute of Low Temperature and Structure Research, Polish Academy of Sciences,
ul. Okólna 2, 50-422 Wrocław, Poland

E-mail: tanya@ie.bas.bg, tatyana_koutzarova@ie.bas.bg

Abstract. We present details of the microstructural properties of Y- ($\text{Ba}_2\text{Mg}_2\text{Fe}_{12}\text{O}_{22}$, $\text{Ba}_{0.5}\text{Sr}_{1.5}\text{Zn}_2\text{Fe}_{12}\text{O}_{22}$, $\text{Ba}_{0.5}\text{Sr}_{1.5}\text{Zn}_2\text{Al}_{0.08}\text{Fe}_{11.92}\text{O}_{22}$) and Z-type ($\text{Sr}_3\text{Co}_2\text{Fe}_{24}\text{O}_{41}$) hexaferrite thick films deposited by screen printing and drop casting on unpolished polycrystalline Al_2O_3 substrates. The hexaferrites thick films obtained by drop casting exhibited considerable roughness and porousness compared with those obtained by screen printing. We found that the powders' morphology significantly affects the microstructure of the thick films formed by screen printing. The microstructural analysis of the thick films shows that their microstructure differs from that of the powders. Further, during the annealing process the grains in the thick films grow and form hexagonal particles, the latter having the largest size, best shape and being best observed in the case of the $\text{Ba}_2\text{Mg}_2\text{Fe}_{12}\text{O}_{22}$ film.

1. Introduction

The magneto-electric coupling in hexaferrites has provoked strong interest due to the opportunities this effect offers in finding novel functional applications. Thus, extensive studies have been launched on finding materials – single-phase, composites, thick or thin films – in which both orderings are simultaneously present. The magneto-electric effect in hexaferrites was found for the first time by T. Kimura and co-authors [1] for a single crystal of $\text{Ba}_{0.5}\text{Sr}_{1.5}\text{Zn}_2\text{Fe}_{12}\text{O}_{22}$ (Y-type hexaferrite) in a magnetic field of about 1 T and at a temperature close to room temperature, with the effect being significant at $T < 130$ K [2]. The $\text{Ba}_2\text{Mg}_2\text{Fe}_{12}\text{O}_{22}$ has a relatively high spiral-magnetic transition temperature (~ 200 K), shows multiferroic properties at zero magnetic field, and the direction of the ferroelectric polarization can be controlled by a small magnetic field (< 0.02 T) [3]. For the first time, the existence of a significant magneto-electric effect in hexaferrites at room temperature was reported by Kitagawa et al. [4], namely, the Z-type hexaferrite $\text{Sr}_3\text{Co}_2\text{Fe}_{24}\text{O}_{41}$ exhibited a low-field (~ 10 mT) magneto-electric effect at room temperature.

⁵ To whom any correspondence should be addressed.



The Y- and Z-types hexaferrites have a complicated crystal structures in comparison with the M-type. The unit cell of Y-type hexaferrite contains three formula units ($Z=3$). The structure can be considered as consisting of two types of crystal S- ($\text{Me}_2\text{Fe}_4\text{O}_8$, spinel block) and T- ($\text{Ba}_2\text{Fe}_8\text{O}_{14}$) blocks consecutively stacked along the hexagonal c axis in the sequence (TST'ST'S'), with the primes indicating rotation about the c -axis by 120 degrees [5]. The Z-type hexaferrites have a very complex crystal structure, being a combination of M-type and Y-type hexaferrites [6]. The unit cell consists of 140 atoms, distributed in S-, R- and T-blocks, which results in a crystal cell with an especially long c -axis length.

Most of the studies having to do with clarifying the causes of the magneto-electric effect existence in hexaferrites have been conducted on single-crystal samples, while from the viewpoint of future applications it is important to obtain new data on this effect in polycrystalline materials, or in thick and thin film structures. The reason why one predominantly finds in the literature data on the magneto-electric effect in single crystals is the difficulty in preparing single-phase specimens of Y- and Z-type hexaferrites. It is known that the temperature intervals for synthesizing different phases of hexaferrites of M-, Y-, Z-, W-, and U-types overlap [5]. Thus, the complex crystal structure and the difficulties in synthesizing Y- and Z-type hexaferrites combine to drive researchers' interest in techniques of forming thick films of already synthesized single-phase powders. From practical application point of view, it is very important to obtain a film with good adhesion and microstructural quality as the microstructure affects to a large extent the film's properties, including the magneto-electric effect. We describe below our studies on the microstructural properties of $\text{Ba}_2\text{Mg}_2\text{Fe}_{12}\text{O}_{22}$, $\text{Ba}_{0.5}\text{Sr}_{1.5}\text{Zn}_2\text{Fe}_{12}\text{O}_{22}$, $\text{Ba}_{0.5}\text{Sr}_{1.5}\text{Zn}_2\text{Al}_{0.08}\text{Fe}_{11.92}\text{O}_{22}$ (Y-type) and $\text{Sr}_3\text{Co}_2\text{Fe}_{24}\text{O}_{41}$ (Z-type) thick films deposited by two different techniques – drop casting and screen printing. An advantage of these two methods is their suitability to producing films with thicknesses from few tens to few hundred microns, thus overcoming the limitation to growing thick films by other deposition techniques; also, no expensive equipment is needed.

2. Experimental

To obtain high-quality thick or thin films, one has to first prepare powders with high homogeneity of the particles' shape and size. The $\text{Ba}_2\text{Mg}_2\text{Fe}_{12}\text{O}_{22}$, $\text{Ba}_{0.5}\text{Sr}_{1.5}\text{Zn}_2\text{Fe}_{12}\text{O}_{22}$, $\text{Ba}_{0.5}\text{Sr}_{1.5}\text{Zn}_2\text{Al}_{0.08}\text{Fe}_{11.92}\text{O}_{22}$ and $\text{Sr}_3\text{Co}_2\text{Fe}_{24}\text{O}_{41}$ samples were synthesized by citric acid sol-gel auto-combustion, as described in our previous publications [7, 8]. The corresponding metal nitrates were used as starting materials and the citric acid was used as a chelator. The solution was slowly evaporated to form a gel, turned into a fluffy mass and burned in a self-propagating combustion manner. The auto-combusted powder was annealed at 600 °C. The precursor powders produced were synthesized at 1170 °C for $\text{Ba}_2\text{Mg}_2\text{Fe}_{12}\text{O}_{22}$, $\text{Ba}_{0.5}\text{Sr}_{1.5}\text{Zn}_2\text{Fe}_{12}\text{O}_{22}$, $\text{Ba}_{0.5}\text{Sr}_{1.5}\text{Zn}_2\text{Al}_{0.08}\text{Fe}_{11.92}\text{O}_{22}$. To prepare $\text{Sr}_3\text{Co}_2\text{Fe}_{24}\text{O}_{41}$, the precursor powder was synthesized at 1200 °C for seven hours and then quenched rapidly to room temperature to form a single-phase material.

Using drop casting, the thick film was deposited from a suspension containing $\text{Ba}_{0.5}\text{Sr}_{1.5}\text{Zn}_2\text{Fe}_{12}\text{O}_{22}$ or $\text{Sr}_3\text{Co}_2\text{Fe}_{24}\text{O}_{41}$ powder. The suspension was made by dispersing hexaferrite particles into a polyvinyl alcohol solution (PVA) and dropped on the polycrystalline Al_2O_3 substrates. The as-deposited samples were slowly dried and annealed for five hours at 1170 °C in the case of $\text{Ba}_{0.5}\text{Sr}_{1.5}\text{Zn}_2\text{Fe}_{12}\text{O}_{22}$ film and at 1200 °C in the case of $\text{Sr}_3\text{Co}_2\text{Fe}_{24}\text{O}_{41}$ film.

For screen printing, the suspensions were made by homogeneously dispersing the corresponding Y-hexaferrite powders in varnish, and Z-hexaferrite powders in a PVA solution or in varnish. The prepared suspensions were screen printed on unpolished polycrystalline Al_2O_3 substrates. The as-deposited samples were slowly dried and annealed at 1170 °C for 30 min.

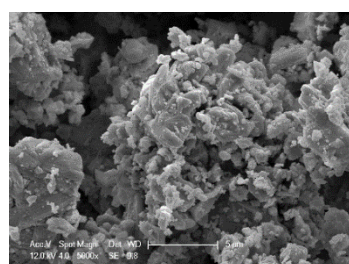
The powders and the thick films were characterized using X-ray diffraction with Cu-K α radiation. The microstructure of the samples was observed by scanning electron microscopy (Philips ESEM XL30 FEG and JEOL 6390).

3. Results and discussion

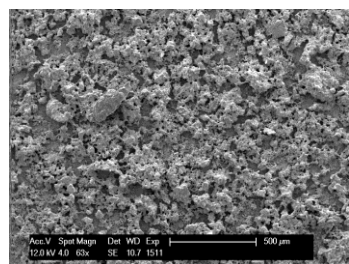
The X-ray phase analysis of the powder samples and the thick films showed the presence of only Ba₂Mg₂Fe₁₂O₂₂, Ba_{0.5}Sr_{1.5}Zn₂Fe₁₂O₂₂, Ba_{0.5}Sr_{1.5}Zn₂Al_{0.08}Fe_{11.92}O₂₂ and Sr₃Co₂Fe₂₄O₄₁.

Figure 1 shows SEM images of the Ba_{0.5}Sr_{1.5}Zn₂Fe₁₂O₂₂ powder and the corresponding thick film produced by drop casting. The thick films show considerable roughness and porosity. The shapes and sizes of the grains in the films are different from those in the initial powder used for casting. A melting process was also observed. Figure 2 shows SEM images of a Ba_{0.5}Sr_{1.5}Zn₂Fe₁₂O₂₂ thick film prepared by screen printing deposition of powder admixed in varnish. The roughness and porosity of the film surface are lower than those in the case of drop casting. During the high-temperature annealing, the grains in the thick films grow and form hexagonal particles. Similar results are observed for Ba₂Mg₂Fe₁₂O₂₂ and Ba_{0.5}Sr_{1.5}Zn₂Al_{0.08}Fe_{11.92}O₂₂ thick films formed by screen printing (figure 3). The largest size and best hexagonal shape are seen in the case of the Ba₂Mg₂Fe₁₂O₂₂ film, where the thickness of the grains is less than 350 nm (figure 3c).

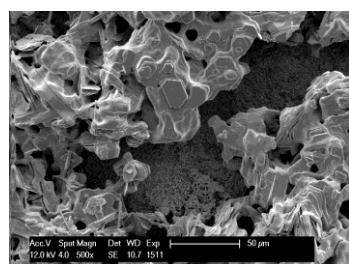
In our previous work [8], we reported the results of microstructural analysis of Sr₃Co₂Fe₂₄O₄₁



a)



b)



c)

Figure 1 (see the column to the left). SEM images of Ba_{0.5}Sr_{1.5}Zn₂Fe₁₂O₂₂ (a) powder and (b, c) thick films obtained by drop casting.

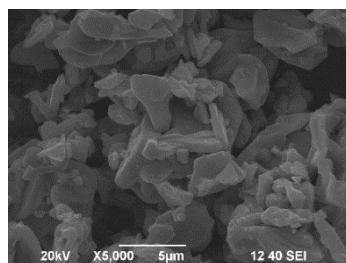
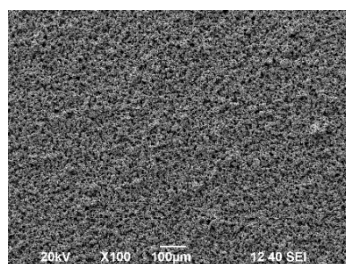


Figure 2. SEM images of Ba_{0.5}Sr_{1.5}Zn₂Fe₁₂O₂₂ thick films obtained by screen printing.

thick films prepared by drop casting, which exhibited a considerable roughness similar to that of the Ba_{0.5}Sr_{1.5}Zn₂Fe₁₂O₂₂ thick film. Also, the particles had the perfect hexagonal shape typical for hexaferrites. Figure 4 presents the SEM images of Sr₃Co₂Fe₂₄O₄₁ thick films prepared by screen printing deposition from PVA paste resulting in very bad coverage; thus, it is not a technique suitable for forming Sr₃Co₂Fe₂₄O₄₁ thick films. However, the grains have grown to a hexagonal shape, in contrast with the grains in the powder used for preparing the suspension. The thickness of the grain is between 200-350 nm. Figure 5 shows SEM images of the Sr₃Co₂Fe₂₄O₄₁ powder and the corresponding thick film obtained by screen printing of powder admixed in varnish. The particles' shapes and size in the films are different than those of the precursor powder. The surface morphology of the thick film is characterized by a lower degree of roughness compared with the ones discussed before, but not a sufficiently well-expressed hexagonal shape of the grains.

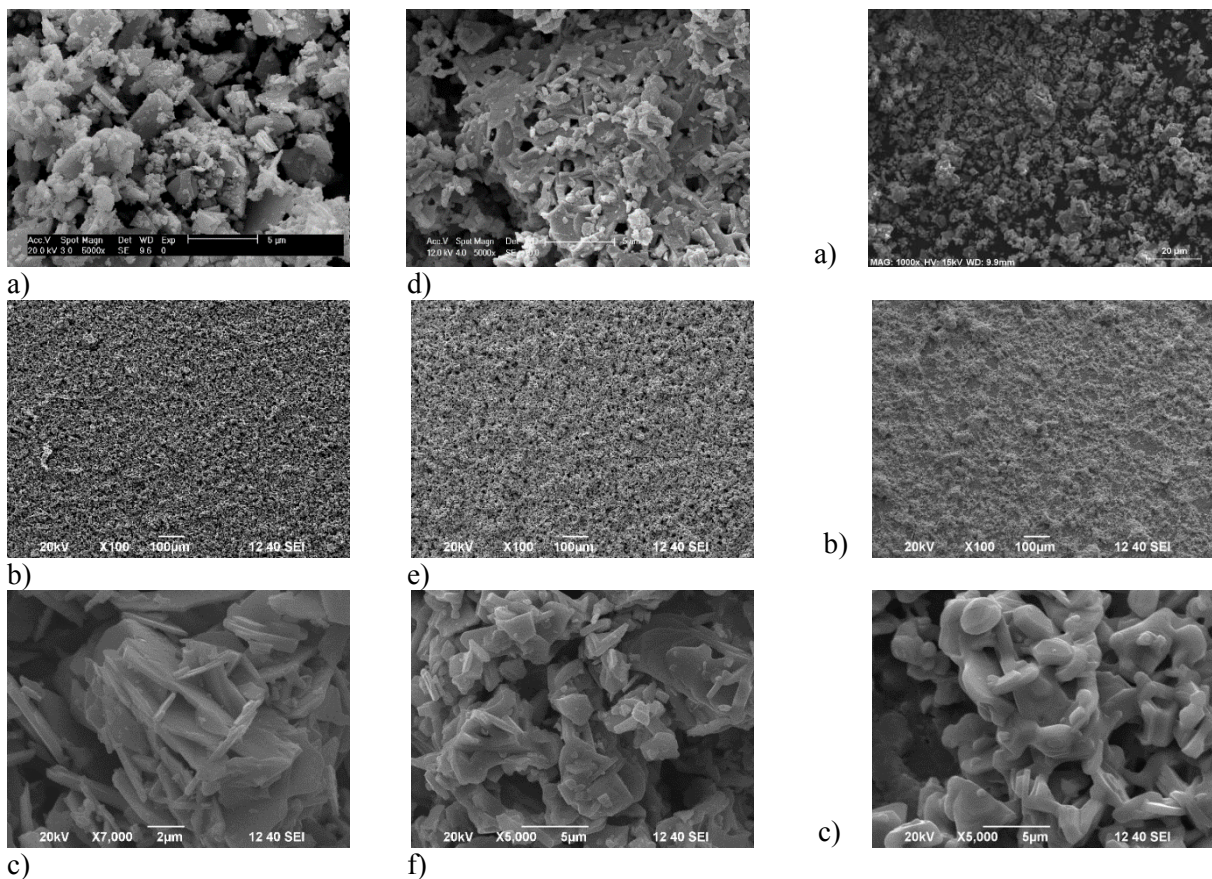


Figure 3. SEM images of $\text{Ba}_2\text{Mg}_2\text{Fe}_{12}\text{O}_{22}$ (a) and $\text{Ba}_{0.5}\text{Sr}_{1.5}\text{Zn}_2\text{Al}_{0.08}\text{Fe}_{11.92}\text{O}_{22}$ (d) powders, and (b, c) $\text{Ba}_2\text{Mg}_2\text{Fe}_{12}\text{O}_{22}$ thick film and (e, f) $\text{Ba}_{0.5}\text{Sr}_{1.5}\text{Zn}_2\text{Al}_{0.08}\text{Fe}_{11.92}\text{O}_{22}$ thick film prepared by screen printing deposition of powder admixed in varnish.

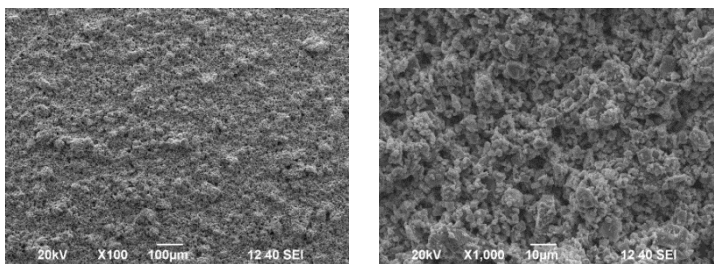


Figure 5. SEM images of $\text{Sr}_3\text{Co}_2\text{Fe}_{24}\text{O}_{41}$ thick films prepared by screen printing deposition of powder admixed in varnish.

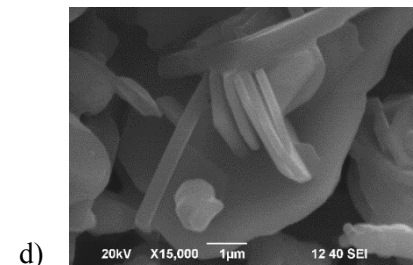


Figure 4. SEM images of $\text{Sr}_3\text{Co}_2\text{Fe}_{24}\text{O}_{41}$ (a) powder and (b, c) thick films prepared by screen printing deposition of powder admixed in PVA.

4. Conclusions

$\text{Ba}_2\text{Mg}_2\text{Fe}_{12}\text{O}_{22}$, $\text{Ba}_{0.5}\text{Sr}_{1.5}\text{Zn}_2\text{Fe}_{12}\text{O}_{22}$, $\text{Ba}_{0.5}\text{Sr}_{1.5}\text{Zn}_2\text{Al}_{0.08}\text{Fe}_{11.92}\text{O}_{22}$ and $\text{Sr}_3\text{Co}_2\text{Fe}_{24}\text{O}_{41}$ thick films were prepared by drop casting and screen printing. The hexaferrites thick films produced by drop casting are considerably more rough and porous compared with those formed by screen printing. The screen printing deposition from PVA paste results in a very bad coverage, i.e., using PVA as solvent is not suitable for depositing $\text{Sr}_3\text{Co}_2\text{Fe}_{24}\text{O}_{41}$ thick films. The only advantage of using PVA is that it enhances the processes of grain growth to a hexagonal shape, even after a very short high-temperature annealing. The powder's morphology significantly affects the microstructure of the thick films formed by screen printing. The microstructural analysis of the thick films show that their microstructure

differs from that of the powders and during the annealing process the grains in the thick films grow and form hexagonal particles, the latter having the largest size, best shape and being best observed in the case of the $\text{Ba}_2\text{Mg}_2\text{Fe}_{12}\text{O}_{22}$ film.

Acknowledgments

The work was supported by the Bulgarian National Science Fund under contract DN 08/4 “Novel functional ferrites-based magneto-electric structures” and a joint research project between Bulgarian Academy of Sciences and WBI, Belgium. B. Georgieva’s work on sample $\text{Ba}_{0.5}\text{Sr}_{1.5}\text{Zn}_2\text{Al}_{0.08}\text{Fe}_{11.92}\text{O}_{22}$ was supported by the Bulgarian Ministry of Education and Science under the National Research Program “Young scientists and postdoctoral students” approved by DCM # 577/17.08.2018.

References

- [1] Kimura T, Lawes G and Ramirez AP 2005 *Phys. Rev. Lett.* **94** 137201
- [2] Utsumi S, Yoshida D and Momozawa N 2007 *J. Phys. Soc. Jpn.* **76** 034704
- [3] Taniguchi K, Abe N, Ohtani S, Umetsu H and Arima T 2008 *Appl. Phys. Express* **1** 031301
- [4] Kitagawa Y, Hiraoka Y, Honda T, Ishikura T, Nakamura H and Kimura T 2010 *Nat. Mater.* **9** 797
- [5] Pullar R C 2012 *Prog. Mater. Sci.* **57** 1191-334
- [6] Mu Ch, Song Y, Wang L and Zhang H 2011 *J. Appl. Phys.* **109** 123925
- [7] Georgieva B, Kolev S, Krezhov K, Ghelev Ch, Kovacheva D, Vertruyen B, Closset R, Tran LM, Babij M, Zaleski A and Koutzarova T 2019 *J. Magn. Magn. Mater.* **477** 131
- [8] Koutzarova T, Ghelev Ch, Peneva P, Georgieva B, Kolev S, Vertruyen B and Closset R 2018 *J. Phys.: Conf. Ser.* **992** 012058